Chapter 2
Phasor Estimation of Nominal Frequency Inputs

2.1 Phasors of Nominal Frequency Signals

Consider a constant input signal $x(t)$ at the nominal frequency of the power system f_0, which is sampled at a sampling frequency Nf_0. The sampling angle θ is equal to $2\pi/N$, and the phasor estimation is performed using Eqs. (1.25)–(1.27).

$$x(t) = X_m \cos(2\pi f_0 t + \phi) \tag{2.1}$$

The N data samples of this input x_n:{n = 0, 1, 2, …, N − 1) are

$$x_n = X_m \cos(n\theta + \phi) \tag{2.2}$$

Since the principal interest in phasor measurements is to calculate the fundamental frequency component, we will set k = 1 in Eqs. (1.25)–(1.27) to produce the fundamental frequency phasor obtained from the sample set x_n. The superscript (N − 1) is used to identify the phasor as having the (N − 1)st sample as the last sample used in the phasor estimation.

$$\begin{aligned} X_c^{N-1} &= \frac{\sqrt{2}}{N}\sum_{n=0}^{N-1} x_n \cos(n\theta) = \frac{\sqrt{2}}{N}\sum_{n=0}^{N-1} X_m \cos(n\theta+\phi)\cos(n\theta) \\ &= \frac{\sqrt{2}}{N} X_m \sum_{n=0}^{N-1}\left[\cos(\phi)\cos^2(n\theta) - \frac{1}{2}\sin(\phi)\sin(2n\theta)\right] = \frac{X_m}{\sqrt{2}}\cos(\phi) \end{aligned} \tag{2.3}$$

It is to be noted that the summation of the $\sin(2n\theta)$ term over one period is identically equal to zero, and that the average of the $\cos^2(n\theta)$ term over a period is equal to 1/2.

A.G. Phadke and J.S. Thorp, *Synchronized Phasor Measurements and Their Applications*, Power Electronics and Power Systems,
DOI 10.1007/978-3-319-50584-8_2

The sine sum is calculated in a similar fashion:

$$\begin{aligned} X_s^{N-1} &= \frac{\sqrt{2}}{N}\sum_{n=0}^{N-1} x_n \sin(n\theta) = \frac{\sqrt{2}}{N}\sum_{n=0}^{N-1} X_m \cos(n\theta+\phi)\sin(n\theta) \\ &= \frac{\sqrt{2}}{N} X_m \sum_{n=0}^{N-1}\left[\frac{1}{2}\cos(\phi)\sin(2n\theta) - \sin(\phi)\sin^2(n\theta)\right] \\ &= -\frac{X_m}{\sqrt{2}}\sin(\phi) \end{aligned} \tag{2.4}$$

The phasor X^{N-1} is given by

$$X^{N-1} = X_c^{N-1} - jX_s^{N-1} = \frac{X_m}{\sqrt{2}}[\cos(\phi) + j\,\sin(\phi)] = \frac{X_m}{\sqrt{2}}e^{j\phi} \tag{2.5}$$

It is to be understood that Eq. 2.5 gives the fundamental frequency phasor estimate, even though the subscript $k = 1$ has been dropped for the sake of simplicity. The result obtained in Eq. (2.5) conforms with the phasor definition given in Chap. 1, and the phase angle ϕ of the phasor is the angle between the time when the first sample is taken (corresponding to $n = 0$) and the peak of the input signal.

2.2 Formulas for Updating Phasors

2.2.1 Non-recursive Updates

Considering that the phasor calculation is a continuous process, it is necessary to consider algorithms which will update the phasor estimate as the newer data samples are acquired. When the Nth sample is acquired after the previous set of samples has led to the phasor estimate given by Eq. (2.5), the simplest procedure would be to repeat the calculations implied in Eqs. (2.3)–(2.5) for the new data window which begins at $n = 1$ and ends at $n = N$.

$$\begin{aligned} X^{N-1} &= \frac{\sqrt{2}}{N}\sum_{n=0}^{N-1} x_n[(\cos(n\theta) - j\,\sin(n\theta)] \\ X^{N} &= \frac{\sqrt{2}}{N}\sum_{n=0}^{N-1} x_{n+1}[(\cos(n\theta) - j\,\sin(n\theta)] \end{aligned} \tag{2.6}$$

The two windows are shown in Fig. 2.1. Phasor 1 is the result of phasor estimation over window 1, while phasor 2 is calculated with the data in window 2. The first sample in window 1 is lagging the peak of the sinusoid by an angle ϕ, while the

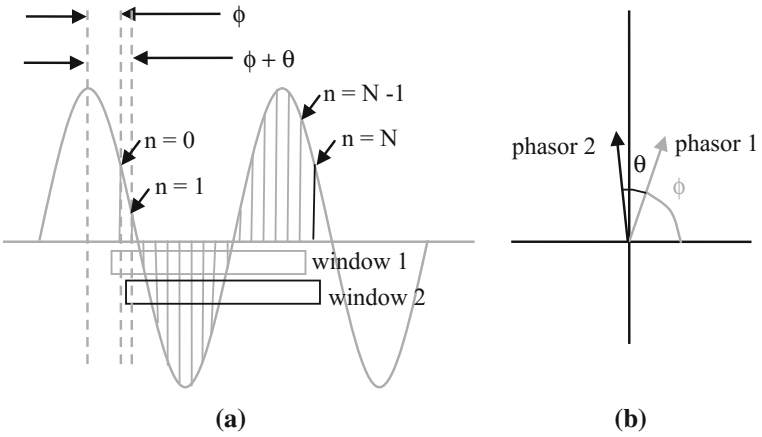

Fig. 2.1 Update of phasor estimates with N sample windows. Phasor 1 is calculated with samples $n = 0, \ldots, N - 1$, while phasor 2 is calculated with samples $n = 1, 2, \ldots N$. θ is the angle between successive samples based on the period of the fundamental frequency

first sample of window 2 ($n = 1$) lags the peak by an angle ($\phi + \theta$), θ being the angle between samples.

It should be clear from Fig. 2.1 that in general, the phasor obtained from a constant sinusoid of nominal power system frequency by this technique will have a constant magnitude and will rotate in the counter-clockwise direction by angle θ as the data window advances by one sample. Since the phasor calculations are performed fresh for each window without using any data from the earlier estimates, this algorithm is known as a *non-recursive algorithm*. Non-recursive algorithms are numerically stable but are somewhat wasteful of computation effort as will be seen in the following.

Figure 2.2 is another view of the non-recursive phasor estimation process. As newer samples are obtained, the table of sine and cosine multipliers is moved down to match the new data window. In this figure, the multipliers are viewed as samples of unit magnitude sine and cosine waves at the nominal power system frequency. The new data window has $N - 1$ samples in common with the old data window. In actual computation, these are simply stored as tables of sine and cosine, which are used repeatedly on each window as needed.

2.2.2 *Recursive Updates*

The formulas for calculating the $(N - 1)$th and (N)th phasors by the non-recursive algorithm are

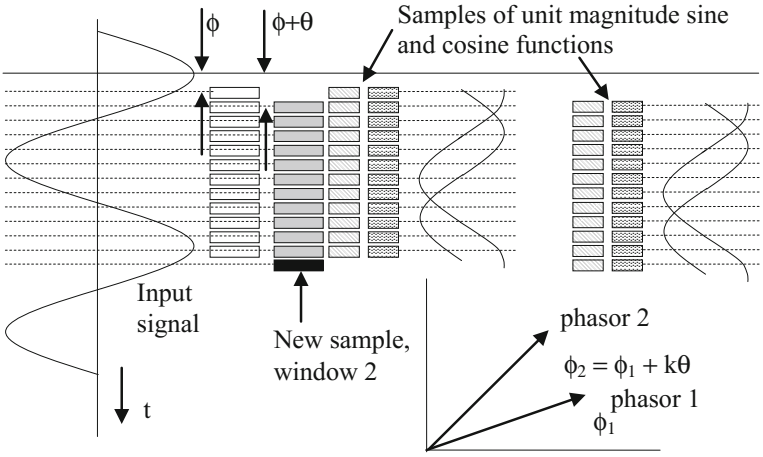

Fig. 2.2 Non-recursive phasor estimation. There are 12 samples per cycle of the power frequency in this example. Fresh calculations are made for each new window as new samples are obtained. The phasor for a constant input signal rotates in the counter-clockwise direction by the sampling angle, in this 30°

$$X^{N-1} = \frac{\sqrt{2}}{N}\sum_{n=0}^{N-1} x_n e^{-jn\theta}$$
$$X^{N} = \frac{\sqrt{2}}{N}\sum_{n=0}^{N-1} x_{n+1} e^{-jn\theta} \tag{2.7}$$

The multipliers for a given sample are different in the two computations. For example, the multiplier for (n = 2) sample in the first sum is $e^{-j2\theta}$, while the multiplier for the same sample in the second sum is $e^{-j\theta}$.

It should be noted that samples x_n: {n = 1, 2, …, N − 1) are common to both windows. The second window has no x_0, so that it begins with x_1, and it ends with x_N, which did not exist in the first window. If one could arrange to keep the multipliers for the common samples the same in the two windows, one would save considerable computations in calculating X^N. If we multiply both sides of the second equation in (2.6) by $e^{-j\theta}$, we obtain the following result:

$$\hat{X}^{N} = e^{-j\theta}X^{N} = \frac{\sqrt{2}}{N}\sum_{n=0}^{N-1} x_{n+1} e^{-j(n+1)\theta}$$
$$= X^{N-1} + \frac{\sqrt{2}}{N}(x_N - x_0)e^{-j(0)\theta} \tag{2.8}$$

where use has been made of the fact that $e^{-j(0)\theta} = e^{-jN\theta}$, since N samples span exactly one period of the fundamental frequency. The phasor defined by Eq. (2.7)

differs from the non-recursive estimate by an angular retardation of θ. The advantage of using this alternative definition for the phasor from the new data window is that $(N - 1)$ the multiplications by the Fourier coefficients in the new window are the same as those used in the first window. Only a recursive update on the old phasor needs to be made to determine the value of the new phasor. This algorithm is known as the *recursive algorithm* for estimating phasors. In general, when the last sample in the data window is $(N + r)$, the recursive phasor estimate is given by

$$\begin{aligned} \widehat{X}^{N+r} &= \mathrm{e}^{-j\theta} X^{N+r-1} + \frac{\sqrt{2}}{N}(x_{N+r} - x_r)\mathrm{e}^{-jr\theta} \\ &= \widehat{X}^{N+r-1} + \frac{\sqrt{2}}{N}(x_{N+r} - x_r)\mathrm{e}^{-jr\theta} \end{aligned} \tag{2.9}$$

When the input signal is a constant sinusoid, x_{N+r} is the same as x_r, and the second term in Eq. (2.8) disappears. The phasor estimate with data from the new window is the same as the phasor estimate with data from the old window when the input signal is a constant sinusoid. In general, the recursive algorithm is numerically unstable. Consider the effect of an error in the estimate from one window—for example, caused by a round-off error. This error is always present in all the phasor estimates from then on. This property of the recursive phasor algorithms must be kept in mind when practical implementation of these algorithms is performed [1]. Nevertheless, because of the great computational efficiency of the recursive algorithm, it is usually the algorithm of choice in many applications.

Unless stated otherwise explicitly, we will assume that only the recursive form of the phasor estimation algorithm is in use (Fig. 2.3).

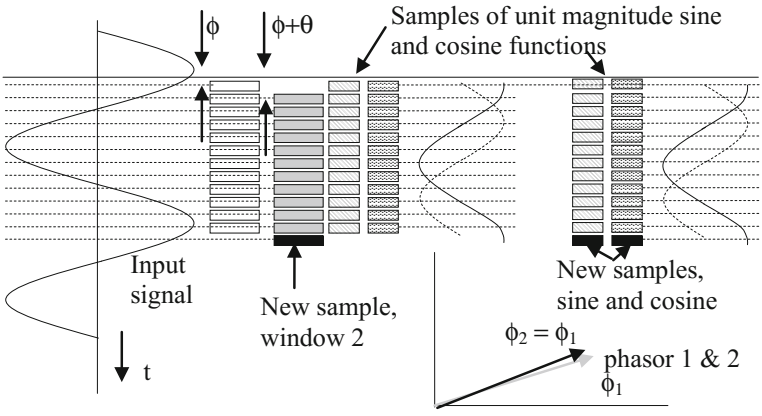

Fig. 2.3 Recursive phasor estimation. There are 12 samples per cycle of the power frequency in this example. Fresh calculations are made for each new window as new samples are obtained. New sine and cosine multipliers are used on the new sample. The phasor for a constant input signal remains stationary

Example 2.1 Consider the 60 Hz signal

$$x(t) = 100\cos(120\pi t + \pi/4)$$

sampled at the rate of 12 samples per cycle, i.e., at a sampling frequency of 720 Hz. The first 18 samples, and the non-recursive and recursive phasor estimates obtained using Eqs. (2.6) and (2.8) beginning with sample no. 12 (at which time the first data window is completely filled) are shown in the following (Table 2.1).

As expected, the non-recursive phasor estimates produce a constant magnitude of $100/\sqrt{2}$ with an initial angle of $\pi/4$ (45°), and then for each successive estimate, the angle increases by 30°.

2.3 Effect of Signal, Noise, and Window Length

The input signals are rarely free from noise. A spurious frequency component which is not a harmonic of the fundamental frequency signal may be considered to be noise. One may also have induced electrical noise picked up in the wiring of the input signal. Leakage effect caused by the windowing function has already been discussed in Chap. 1, and it too contributes to an error in phasor estimation and should therefore be considered as a type of noise in the input.

Table 2.1 Phasor estimates of sampled data

Sample No.	Sample x_n	Non-recursive phasor estimate	Recursive phasor estimate
0	70.7107		
1	25.8819		
2	−25.8819		
3	−70.7107		
4	−96.5926		
5	−96.5926		
6	−70.7107		
7	−25.8819		
8	25.8819		
9	70.7107		
10	96.5926		
11	96.5926		
12	70.7107	70.701∠45°	70.701∠45°
13	25.8819	70.701∠75°	70.701∠45°
14	−25.8819	70.701∠105°	70.701∠45°
15	−70.7107	70.701∠135°	70.701∠45°
16	−96.5926	70.701∠165°	70.701∠45°
17	−96.5926	70.701∠195°	70.701∠45°

As an approximation, we will consider the noise in the input signal to be a zero mean, Gaussian noise process. This should be a good approximation for the electrical noise picked up in the wiring and signal conditioning circuits. The other two sources of noise, viz. non-harmonic frequency components and leakage phenomena need further consideration. A phasor measurement system may be placed in an arbitrarily selected substation and will be exposed to input signals generated by the power system which is likely to change states all the time. Each of the power system states may lead to different non-harmonic frequencies and leakage effects, and the entire ensemble of conditions to which the phasor measurement system is exposed may also be considered to be a pseudo-random Gaussian noise process.

Consider a set of noisy measurement samples

$$x_n = X_m \cos(n\theta + \phi) + \varepsilon_n, \quad \{n = 0, 1, 2, \ldots, N-1\} \tag{2.10}$$

where ε_n is a zero-mean Gaussian noise process with a variance of σ^2. If we set $(X_m/\sqrt{2})\cos(\phi) = X_r$ and $(X_m/\sqrt{2})\sin(\phi) = X_i$, the phasor representing the sinusoid is $X = X_r + jX_i$. We may pose the phasor estimation problem as one of the findings—the unknown phasor estimate from the sampled data through a set of N overdetermined equations:

$$\begin{bmatrix} x_0 \\ x_1 \\ x_2 \\ \cdot \\ x_{N-1} \end{bmatrix} = \sqrt{2} \begin{bmatrix} \cos(0) & -\sin(0) \\ \cos(\theta) & -\sin(\theta) \\ \cos(2\theta) & -\sin(2\theta) \\ \cdot & \cdot \\ \cos[(N-1)\theta] & -\sin[(N-1)\theta) \end{bmatrix} \begin{bmatrix} X_r \\ X_i \end{bmatrix} + \begin{bmatrix} \varepsilon_1 \\ \varepsilon_2 \\ \varepsilon_3 \\ \cdot \\ \varepsilon_{N-1} \end{bmatrix} \tag{2.11}$$

or, in matrix notation

$$[x] = [S][X] + [\varepsilon] \tag{2.12}$$

Assuming that the covariance matrix W of the error vector is σ^2 multiplied by a unit matrix

$$[W] = \sigma^2[1] \tag{2.13}$$

the weighted least squares solution of Eq. (2.11) provides the estimate for the phasor

$$[\widehat{X}] = [S^T W^{-1} S]^{-1} S^T W^{-1} [x] \tag{2.14}$$

Using (2.13) for W, and calculating $\{S^T S\}^{-1}$ for the S in Eq. (2.11):

$$[\widehat{X}] = [S^T W^{-1} S]^{-1} [S^T W^{-1}][x] = [S^T S]^{-1} [S^T][x] = \frac{1}{N}[S^T][x] \tag{2.15}$$

Since the noise is a zero-mean process, the estimate given by (2.15) is unbiased, and the expected value of the estimate is equal to the true value of the phasor. If X is the true value of the phasor, the covariance matrix of the error in the phasor estimate is

$$E\left[[\hat{X} - X][\hat{X} - X]^T\right] = [S^T W^{-1} S]^{-1} \tag{2.16}$$

Substituting for $[W]$ from Eq. (2.13), the covariance of the error in phasor estimate is (σ^2/N). The standard deviations of error in real and imaginary parts of the phasor estimate are $(\sigma/\sqrt{N})$. We may thus conclude that higher sampling rates will produce improvement in phasor estimates in inverse proportion of the square root of the number of samples per cycle. Alternatively, if longer data windows are used (multiple of cycles), then once again the errors in phasor estimate go down as the square root of the number of cycles used. Thus, a four cycle phasor estimate is twice as accurate as a one cycle estimate in with noisy input.

Example 2.2 Consider a 60 Hz sinusoid

$$x(t) = 100\cos(120\pi t + \pi/4) + \varepsilon(t)$$

in a noisy environment, with the Gaussian noise ε having a zero mean and a standard deviation of 1. The source of noise could be electromagnetic interference, quantization errors, or harmonic and non-harmonic components in the input signal. If the phasing of the harmonic and non-harmonic signals is random, the noise model may be approximated by a zero-mean Gaussian characteristic.

The signal is sampled at six different sampling rates: 8, 16, 32, 64, 128, and 256 times per cycle. The signal samples are created with appropriately modeled noise input for 1000 cycles, and 1000 estimates of the phasor value are calculated. The standard deviations of the errors in the 1000 phasor estimates as well as its theoretical value $(\sigma/\sqrt{N})$ are given in Table 2.2 and are also shown in Fig. 2.4.

These results show very good agreement with the expected results. As mentioned earlier, increasing the data window size at a fixed sampling rate, rather than the number of samples in the same data window will produce similar results.

Table 2.2 Phasor estimation of a noisy signal

No. of samples per cycle N	Standard deviation of input noise	Standard deviation of phasor estimate error (volts)	$\sigma/\sqrt{N}$
8	1	0.3636	0.3536
16	1	0.2601	0.2500
32	1	0.1794	0.1768
64	1	0.1231	0.1250
128	1	0.0880	0.0884
256	1	0.0626	0.0625

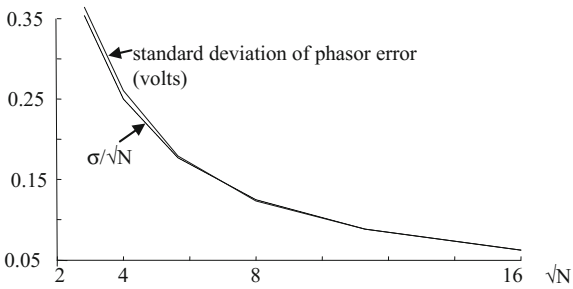

Fig. 2.4 Standard deviation of phasor error due to zero-mean Gaussian noise in the input. The result of 1000 phasor estimates at each sampling rate is shown by the solid line, and the theoretical value of the standard deviation ($\sigma/\sqrt{N}$) is shown by the *dotted line*

2.3.1 Errors in Sampling Times

Another possible source of error in input data samples is the error in timing of the sampling pulses. One possible source of errors is that the sampling clock is not precisely at a multiple of the power system frequency. This case will be dealt with in the next chapter, when we consider the phasor estimation problem at off-nominal frequencies.

In this section, we will consider the case where the sample times are corrupted by a Gaussian random noise with standard deviation varying by up to 10% of the sampling interval. Large errors of this type should not exist in modern measuring systems. Nevertheless, when sampling pulses are generated with the help of software clocks, it is possible to encounter random errors in sampling times. The following numerical example considers errors of this type. The errors are truncated at 3 times the standard deviation in order to eliminate impossibly large sampling clock errors.

Example 2.3 Consider a 60 Hz sinusoid

$$x(t) = 100\cos(120\pi t + \pi/4)$$

which is sampled at $t_n = n\Delta T + \varepsilon$, where the Gaussian noise ε has a zero mean and a standard deviation of $b\Delta T$, with the parameter b varying between 0.0 and 0.10. The signal is sampled at a sampling rate of 32 times per cycle. The signal samples are created with sampling time errors for 1000 cycles, and 1000 estimates of the phasor value are calculated. The standard deviations of the errors in the 1000 phasor estimates are given in Table 2.3 and are also shown in Fig. 2.5.

2.4 Phasor Estimation with Fractional Cycle Data Window

The weighted least squares solution technique developed in Sect. 2.2 is a convenient vehicle for calculating phasors from fractional cycle data windows. It should be remembered that fractional cycle phasor estimates are necessary in developing

Table 2.3 Errors in phasor estimation due to noisy inputs

Coefficient '*b*' of input noise described above	Standard deviation of phasor estimate error (volts)
0.00	0.0000
0.02	0.0705
0.04	0.1373
0.06	0.2111
0.08	0.2809
0.10	0.3432

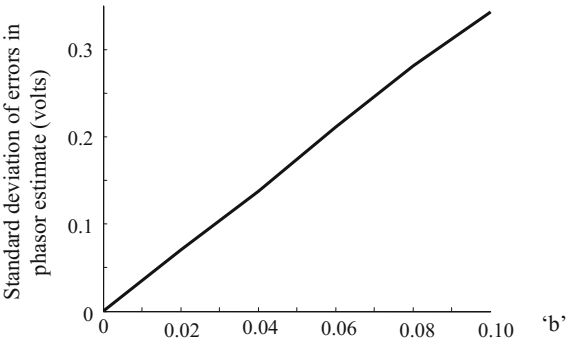

Fig. 2.5 Standard deviation of phasor error due to zero-mean Gaussian noise in sampling clock pulses. The result of 1000 phasor estimates at different values of 'b' coefficients are shown

high speed relaying applications, and not particularly useful in wide area phasor measurement applications whereby measurement times of a few cycles are acceptable. Nevertheless, it is instructive to include a discussion of fractional cycle phasor estimation.

Consider the use of M samples of a sinusoid for estimating phasors, the sinusoid having been sampled at a sampling rate of N samples per cycle. $M < N$ produces a fractional cycle phasor estimation algorithm.

As before, the input is set of noisy measurement samples

$$x_n = X_m \cos(n\theta + \phi) + \varepsilon_n, \quad \{n = 0, 1, 2, \ldots, M-1) \tag{2.17}$$

where ε_n is a zero-mean Gaussian noise process with a variance of σ^2. The sampling angle θ is equal to $2\pi/N$.

$$\begin{bmatrix} x_0 \\ x_1 \\ x_2 \\ . \\ x_{M-1} \end{bmatrix} = \sqrt{2} \begin{bmatrix} \cos(0) & -\sin(0) \\ \cos(\theta) & -\sin(\theta) \\ \cos(2\theta) & -\sin(2\theta) \\ . & . \\ \cos[(M-1)\theta] & -\sin[(M-1)\theta) \end{bmatrix} \begin{bmatrix} X_r \\ X_i \end{bmatrix} + \begin{bmatrix} \varepsilon_1 \\ \varepsilon_2 \\ \varepsilon_3 \\ . \\ \varepsilon_{M-1} \end{bmatrix} \tag{2.18}$$

or, in matrix notation

$$[x] = [S][X] + [\varepsilon] \tag{2.19}$$

As before, the weighted least squares solution of Eq. (2.17) provides the estimate for the phasor

$$[\widehat{X}] = [S^T W^{-1} S]^{-1} S^T W^{-1} [x] \tag{2.20}$$

Using (2.13) for W, and calculating $\{S^T S]^{-1}$ for the S in Eq. (2.11):

$$[\widehat{X}] = [S^T W^{-1} S]^{-1} [S^T W^{-1}][x] = [S^T S]^{-1} [S^T][x] \tag{2.21}$$

Unlike in the case of the full cycle phasor estimation, $[\mathrm{S^T S}]^{-1}$ is no longer a simple matrix:

$$[S^T S] = 2 \begin{bmatrix} \sum_{n=0}^{M-1} \cos^2(n\theta) & \sum_{n=0}^{M-1} \cos(n\theta)\sin(n\theta) \\ \sum_{n=0}^{M-1} \cos(n\theta)\sin(n\theta) & \sum_{n=0}^{M-1} \sin^2(n\theta) \end{bmatrix} \tag{2.22}$$

It can be shown that for a half-cycle estimation, with $M = N/2$, the least squares solution is very similar to the DFT estimator.

2.5 Quality of Phasor Estimate and Transient Monitor

Phasor estimates obtained from a data window represent the fundamental frequency component of the input confined to the data window. When a fault occurs on the power system, there is a series of data windows which contain pre- and post-fault data. This is illustrated in Fig. 2.6 for an assumed voltage waveform during a fault.

It should be clear that although a phasor estimate will be available for all data windows (including the ones that are shaded in Fig. 2.6), only phasors which belong entirely to the pre- or post-fault periods are of interest. The phasors computed for the shaded windows of Fig. 2.6 do not represent any meaningful system state, and a technique is needed to detect the occurrence of mixed states within a data window.

A technique known as 'Transient Monitor' [2] provides a measure to indicate a 'quality' of the estimate and can also be used to detect the condition when a data window contains mixed state waveforms. Consider the process of computing the data samples $(\widehat{x}_n)$ in a window from the estimated phasor which has been estimated from a sample set (x_n):

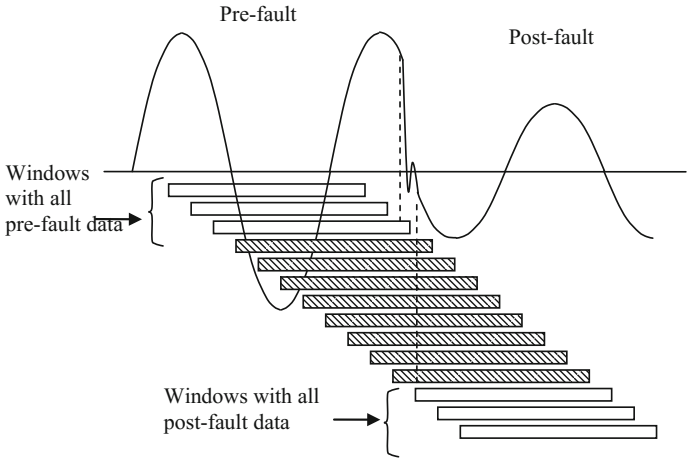

Fig. 2.6 Transition from pre-fault to post-fault waveforms. The *shaded windows* contain mixed waveform data

$$[\widehat{x}_n] = \sqrt{2}\begin{bmatrix} \cos(0) & -\sin(0) \\ \cos(\theta) & -\sin(\theta) \\ \cos(2\theta) & -\sin(2\theta) \\ \cdot & \cdot \\ \cos[(N-1)\theta] & -\sin[(N-1)\theta] \end{bmatrix} \begin{bmatrix} \widehat{X}_r \\ \widehat{X}_i \end{bmatrix} \tag{2.23}$$

Substituting for the phasor estimate from Eq. (2.15)

$$\left[\widehat{x}_n\right] = \sqrt{2}\begin{bmatrix} \cos(0) & -\sin(0) \\ \cos(\theta) & -\sin(\theta) \\ \cos(2\theta) & -\sin(2\theta) \\ \cdot & \cdot \\ \cos[(N-1)\theta] & -\sin[(N-1)\theta] \end{bmatrix} \times \frac{\sqrt{2}}{N}\begin{bmatrix} \cos(0) & \cos(\theta) & \cos(2\theta) & \cdot & \cos[(N-1)\theta) \\ -\sin(0) & -\sin(\theta) & -\sin(2\theta) & \cdot & -\sin[(N-1)\theta) \end{bmatrix}[x_n] \tag{2.24}$$

Multiplying the matrices and simplifying

$$\left[\widehat{x}_n\right] = \frac{2}{N}\begin{bmatrix} 1 & \cos(\theta) & \cos(2\theta) & \cdot & \cos[(N-1)\theta) \\ \cos(\theta) & 1 & \cos(\theta) & \cdot & \cos(0) \\ \cos(2\theta) & \cos(\theta) & 1 & \cdot & \cos(\theta) \\ \cdot & \cdot & \cdot & 1 & \cdot \\ \cos[(N-1)\theta) & \cos(0) & \cos(\theta) & \cdot & 1 \end{bmatrix}[x_n] \tag{2.25}$$

where use has been made of the fact that $N = 2\pi$. The difference between the input data and the re-computed sample data from the phasor estimate is the error of estimation $[t_n]$:

$$[t_n] = [x_n - \widehat{x}_n] = \begin{bmatrix} 1-\frac{2}{N} & -\frac{2}{N}\cos(\theta) & -\frac{2}{N}\cos(2\theta) & \cdot & -\frac{2}{N}\cos[(N-1)\theta] \\ -\frac{2}{N}\cos(\theta) & 1-\frac{2}{N} & -\frac{2}{N}\cos(3\theta) & \cdot & -\frac{2}{N}\cos(0) \\ -\frac{2}{N}\cos(2\theta) & -\frac{2}{N}\cos(3\theta) & 1-\frac{2}{N} & \cdot & -\frac{2}{N}\cos(\theta) \\ \cdot & \cdot & \cdot & 1-\frac{2}{N} & \cdot \\ -\frac{2}{N}\cos[(N-1)\theta] & -\frac{2}{N}\cos(0) & -\frac{2}{N}\cos(\theta) & \cdot & 1-\frac{2}{N} \end{bmatrix} [x_n] \tag{2.26}$$

If the input signal is a pure sinusoid at fundamental frequency, all entries of $[t_n]$ will be identically equal to zero. However, when the input signal is noisy or contains a composite window of two different sinusoids, $[t_n]$ is not zero, and one may use the sum (T_n) of the absolute values of its elements as a measure of the error of estimation.

$$T_n = \sum_{k=0}^{N-1} |t_k| \tag{2.27}$$

This sum has been referred as a 'Transient Monitor' and can be used as a measure of the 'quality' of the phasor estimate.

Example 2.4 Consider a composite 60 Hz voltage waveform samples described by

$$x_n = 100\cos(n\theta + \pi/4), \quad \text{for } n = 0, 1, 2, \ldots, 35$$
$$x_n = 50\cos(n\theta + \pi/8), \quad \text{for } n = 36, 37, 38, \ldots, 71$$

with a sampling rate of 24 samples per cycle; thus, $\theta = \pi/12$.

The data samples, recursive phasor estimates, and the function T_n are shown in Table 2.4.

Note that in the interest of saving space, several rows which do not show interesting transitions have been omitted. The phasor estimates and the transient monitor are plotted in Fig. 2.7.

Note that the phasor estimate remains stationary at $(50 + j50)$ and $(32.6641 + j13.5299)$, while the input signal is $70.7\angle 45°$ and $50\angle 22.5°$, respectively, and the transition from one value to another takes 24 samples, the width of phasor estimation window. The transient monitor provides a good indication of the quality of the phasor estimate, it being high during the transition period when the phasor estimate is unreliable.

Table 2.4 Transient Monitor for a transient signal

Sample No.	Sample value	Phasor	T_n
1	70.7107	0	
2	50.0000	0	
23	96.5926	0	
24	86.6025	50.0 + *j*50.0	0.0000
36	−86.6025	50.0 + *j*50.0	0.0000
37	−46.1940	48.5553 + *j*50.0	51.4677
38	−39.6677	47.9672 + *j*50.1576	67.5480
39	−30.4381	48.1998 + *j*50.0233	68.1205
40	−19.1342	48.9970 + *j*49.2261	80.9808
41	−6.5263	49.9518 + *j*47.5723	129.1521
42	6.5263	50.6149 + *j*45.0978	195.2854
43	19.1342	50.6149 + *j*42.0587	267.1946
44	30.4381	49.7583 + *j*38.8619	331.2446
45	39.6677	48.0811 + *j*35.9570	382.1787
46	46.1940	45.8392 + *j*33.7151	413.6845
47	49.5722	43.4397 + *j*32.3297	430.7721
48	49.5722	41.3320 + *j*31.7650	436.9438
49	46.1940	39.8874 + *j*31.7650	432.8577
50	39.6677	39.2993 + *j*31.9225	426.1713
51	30.4381	39.5318 + *j*31.7883	431.3592
52	19.1342	40.3290 + *j*30.9910	433.7538
53	6.5263	41.2839 + *j*29.3372	424.5001
54	−6.5263	41.9469 + *j*26.8628	405.5234
55	−19.1342	41.9469 + *j*23.8236	367.7588
56	−30.4381	41.0903 + *j*20.6269	314.0214
57	−39.6677	39.4132 + *j*17.7219	243.3327
58	−46.1940	37.1713 + *j*15.4800	162.9157
59	−49.5722	34.7718 + *j*14.0947	77.7374
60	−49.5722	32.6641 + *j*13.5299	0.0000
72	49.5722	32.6641 + *j*13.5299	0.0000

2.6 DC Offset in Input Signals

Fault currents in a power system often have an exponentially decaying dc component, which is generally known as the dc offset. Occasionally, voltage waveforms may also have a dc offset due to capacitive voltage transformer transients. In both cases, the dc offsets decay to negligible values in a few cycles. If the phasor estimate is performed while a dc offset is present in a waveform, one is likely to get significant errors in phasor estimate while the dc offset is nonzero. The transient monitor described in Sect. 2.4 can be used to alert the user that the phasor estimate thus obtained is unreliable.

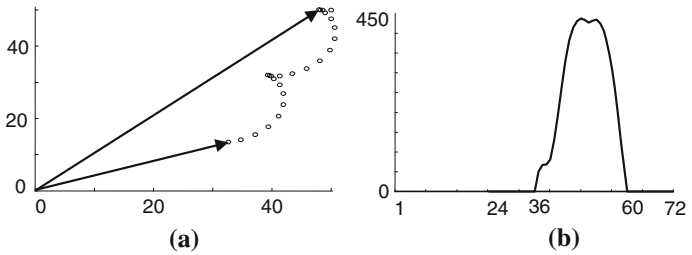

Fig. 2.7 Result of phasor estimation in a data stream with mixed input signals. **a** Phasor estimates. The transition from a solid phasor at 50 + *j*50 to a new phasor of 32.6641 + *j*13.5299 is shown by *open circles*. **b** The transient monitor T_n. Note that it is high during the transition from one phasor value to another. When the input signal is a pure sinusoid, the T_n becomes zero

Since many phasor applications are dedicated to relatively slow phenomena, it is not essential that dc offset be handled in any special way; one only needs to be alert to the estimate quality indicated by the transient monitor. However, in computer relaying applications, powerful techniques have been developed to remove dc offsets before phasors are estimated, and in very specific applications of phasors which require very high speed of response, it may be necessary to employ algorithms which will remove the dc offset from the signals. This section provides a brief summary of the available techniques for this purpose. We will consider only the dc offset in current waveforms when a fault occurs. Similar techniques are applicable to the handling of dc offset in the voltage waveforms as well.

The earliest technique used in relays for removing the dc offset from fault currents is the one of using a 'mimic' circuit in the secondary winding of a current transformer [3]. Figure 2.8 shows the primary fault circuit, and the current transformer secondary winding with a burden ($r + j\omega l$) such that the ratio R/L is matched exactly by the burden ratio r/l. In this case, the dc offset in the current is not present in the voltage $e_2(t)$ across the burden, and the burden voltage can be used as a signal which is proportional to the current and is free from the dc offset. The primary fault circuit and the CT secondary burden are both primarily inductive in nature, and hence, the mimic circuit acts as a differentiator. Thus, it has the property of amplifying any high frequency noise that may be present in the current. However, it should be remembered that the primary fault current is itself is produced by the *R–L* circuit, and thus has attenuated the high frequency noise that may be present in the voltage signal. Thus, although the mimic circuit is a differentiator, the noise content of the voltage across it is similar to that in the primary voltage.

For computer relays, there is a least squares solution technique available for eliminating the dc offset, which is free from the noise amplification properties of the mimic circuit. Consider a fault current $i(t)$, containing a dc offset is given by

$$\begin{aligned} i(t) &= A\cos(\omega t) + B\sin(\omega t) - C\varepsilon^{-t/T} \quad \text{for } t \geq 0 \\ &= A - C \qquad t = 0- \end{aligned} \tag{2.28}$$

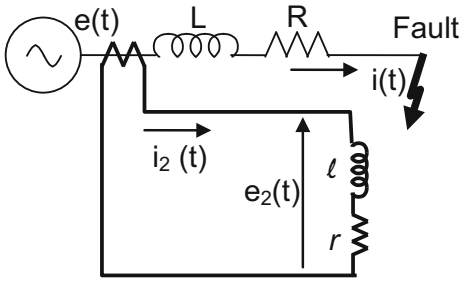

Fig. 2.8 Fault circuit and the mimic burden in CT secondary to eliminate the dc offset in fault current

This expression assumes that the current just before the occurrence of fault is $(A - C)$, and that the dc offset decays with a time constant T, which for the circuit of Fig. 2.8 is equal to L/R seconds.

Consider a sample set of M data points obtained from this current waveform

$$i_n = A\cos(n\theta) + B\sin(n\theta) - \mathrm{Cr}^n, \quad \text{for } \{n = 0, 1, 2, \ldots, M-1) \tag{2.29}$$

where θ is the sampling angle equal to $2\pi/N$, N being the number of samples per cycle of the nominal frequency, and r is the decrement factor for the decaying dc component in one sample time

$$r = \varepsilon^{-\Delta T/T} \tag{2.30}$$

If we now assume that the decrement factor r is known, the only unknowns in Eq. (2.30) are A, B, and C. Taking the overdetermined set of M data points,

$$\begin{bmatrix} i_0 \\ i_1 \\ \\ i_{M-1} \end{bmatrix} = \begin{bmatrix} 1 & 0 & -1 \\ \cos\theta & \sin\theta & -r \\ & & \\ \cos(M-1)\theta & \sin(M-1)\theta & -r^{M-1} \end{bmatrix} \begin{bmatrix} A \\ B \\ C \end{bmatrix} \tag{2.31}$$

As usual, the above equation can be solved for A, B, and C, and then by adding (Cr^{-n}) to each sample of the current, the dc offset can be removed from the waveform.

It is possible that the value of the time constant T is not known exactly and an approximate value must be used for 'r'. The algorithm is tolerant of reasonable errors in the value of 'r', as is seen by the following numerical example.

Example 2.5 Consider a fault current waveform with full dc offset given by

$$i(t) = 100\cos(120\pi t) + 100\sin(120\pi t) - 100\mathrm{e}^{-t/0.05}$$

The current is zero before the occurrence of the fault. The dc offset decay time constant is 50 ms.

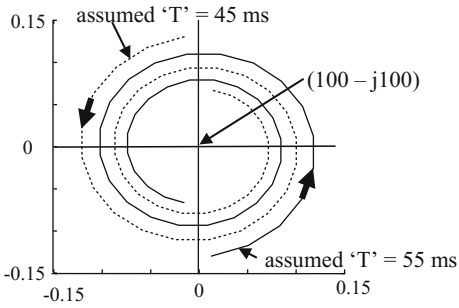

Fig. 2.9 Errors in phasor estimate caused by errors in time constant estimate. Two cycles worth of data are shown. The *solid arrows* show the direction of increasing time

The true value of the phasor must be $(100/\sqrt{2})(1 - j1)$. The dc offset is removed by applying Eq. (2.31) for a window of one cycle at a time. It is assumed that an error of $\pm 10\%$ is made in the decrement factor 'r' used in Eq. (2.31). The resulting error in ($\sqrt{2} \times$ phasor) is shown in Fig. 2.9.

It can be seen from Fig. 2.9 that the errors of estimation of phasors are less than 0.2% even though the time constant errors are of the order of 10%.

The least square solution described above is some times described as a 'digital mimic' procedure. However, it must be pointed out that this process is not a differentiator, and consequently, there is no amplification of noise in the current signal in this process.

2.7 Non-DFT Estimators

A number of papers dealing with the problem of computing phasors from sampled data have been published over the last several years. Several papers consider variations on the Fourier transform method, with special emphasis on the problem of dealing with off-nominal frequency signals. We will consider such signals in the next chapter, where the performance of the fixed frequency Fourier transform on off-nominal frequency input signals will be discussed. Among the variations of the basic Fourier technique, least squares methods, Kalman filter methods, and Prony methods have been discussed. As the main thrust of these variations is to deal with off-nominal frequency signals, we will defer their discussion to a later chapter.

References

1. Phadke, A. G., & Thorp, J. S. (1994). *Computer relaying for power systems* (pp. 127–129). New York: Research Studies Press Ltd., Wiley.
2. ibid. pp. 151–152.
3. Mason, C. R. (1956). *Art and science of protective relaying*. New York: Wiley.

http://www.springer.com/978-3-319-50582-4

Synchronized Phasor Measurements and Their Applications

Phadke, A.G.; Thorp, J.S.

2017, XIII, 285 p. 182 illus., 25 illus. in color., Hardcover
ISBN: 978-3-319-50582-4